JJMIE

Volume 15, Number 1, March. 2021
ISSN 1995-6665
Pages 23 - 27

Jordan Journal of Mechanical and Industrial Engineering

Simulation Analysis of the Effects of EGR Rate on HCCI Combustion of Free-piston Diesel Engine Generator

Chunhui Liu*, Kechuan Yi

College of Mechanical Engineering, Anhui Science and Technology University, Fengyang, Anhui 233100, China

Received July 18 2020 *Accepted Feb 20 2021*

Abstract

The effects of exhaust gas recirculation (EGR) rate on homogeneous charge compression ignition (HCCI) combustion and emission of free-piston diesel engine generator (FPDEG) was investigated by using a three-dimensional (3-D) computational fluid dynamics (CFD) model of FPDEG. In the 3-D CFD model of FPDEG, the diesel mechanism with 109 species and 543 reactions was incorporated into the combustion model, and the soot and NOx production were calculated by Hiroyasu-NSC model and 12 steps NOx model. The simulation results showed that the EGR rate had great influence on the HCCI combustion and emission performance of FPDEG. As the EGR rate was changed from 0 to 10%, the HCCI combustion phase of FPDEG slightly lagged, the peak value of heat release, the maximum in-cylinder temperature and pressure and the NOx content significantly decreased, but SOOT content increased. When the EGR rate was 20%, the HCCI combustion of FPDEG was incomplete, and the UCH, SOOT and CO content all obviously increased.

Keywords: Free-piston diesel engine generator, Homogeneous charge compression ignition, diesel mechanism, exhaust gas recirculation;

1. Introduction

The innovation of energy utilization technology has become an urgent issue due to the growing fossil fuel consumption and environmental pollution. Homogenous charge compression ignition (HCCI) combustion, one of new combustion modes, has been widely investigated owing to its high efficiencies and low emissions [1].

Onishi et al. first introduced HCCI in the experiments of two-stroke gasoline engines [2]. Najt et al. extended HCCI to four-stroke gasoline engines and found that HCCI mainly controlled by chemical kinetics [3]. Ryan et al. conducted the early HCCI combustion research work of diesel fuel and discovered that the operation of diesel HCCI engine mainly relied on EGR rate, compression ratio and air-fuel ratio [4]. Christensen et al. also carried out the research of diesel fuel HCCI combustion and obtained the acceptable ranges of compression ratios and mixture intake temperature [5].

In the recent decades, in addition to conventional internal combustion engines, HCCI is also operated on the free-piston engine generator (FPEG). FPEG has simple structures and high conversion efficiency and can give full play to the advantages of HCCI combustion [6, 7]. Bergman and Fredriksson integrated one-dimensional gas dynamics, SENKIN chemical kinetics, and KIVA-3V CFD simulation platform to compare the HCCI combustion of FPEC and combustion of conventional diesel engines and found the optimal working conditions [8]. Chiang et al. [9] presented the simulation research of a spark ignition (SI)/HCCI FPEG with electric mechanical valves.

Exhaust gas recirculation (EGR) is one of the most effective means to control the ignition time and combustion progress of HCCI. Tsolakis et al. [10] conducted the experiments of EGR system in a diesel engine, and found that EGR can effectively reduce smoke and NOx emissions. Jamal et al. came to the same conclusion as Tsolakis [11]. Yap et al. [12] found that EGR can affect the HCCI combustion characteristics of fuel and then control the ignition time.

It is necessary to choose the precise chemical reactions to study the HCCI combustion of diesel fuel. Nowadays, there exists a lot of chemical models of diesel surrogates. Previously, n-heptane, a single-component surrogate, has been proposed to represent diesel fuel [13]. However, the drawbacks of single-component surrogate are obvious. Currently, multi-component surrogate models, including the aromatic components, have been proposed for diesel fuel [14].

In this paper, the 3-D CFD FPDEG model coupling the 109 species detailed diesel mechanism was created to investigate the effects of EGR rate on HCCI combustion and emission performance.

2. 3D CFD modeling and verification

The key to modeling is to obtain the piston motion law of FPDEG. The method of zero-dimensional models to calculate the piston motion law of FPEG can be found in literature [15].

* Corresponding author e-mail: lch994211@163.com.

The main simulation parameters of CFD model are as follows: the bore is 60 mm, the maximum effective stroke is 61.5 mm, the maximum total stroke is 98 mm and the moving mass of the piston assembly is 6 kg. **Figure 1** displays the moving mesh model of FPDEG combustion chamber. The number range of the structural cartesian grid of the moving mesh model was 14620-1340888. The boundary condition of temperature defined of cylinder wall, cylinder head and position was 450 K, 500 K and 550 K separately.

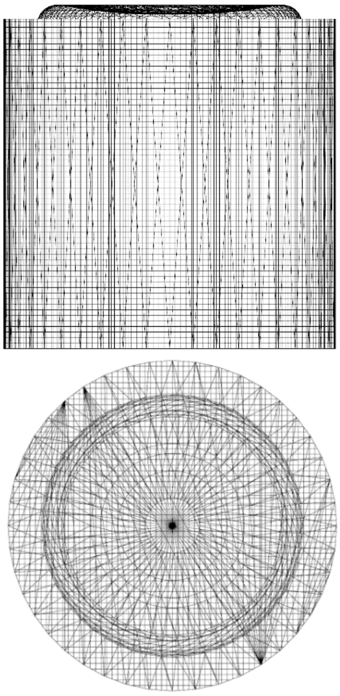

Figure 1. The moving mesh model of FPDEG combustion chamber

The 109 species and 543 elementary reactions mechanism of diesel developed by Wang was adopted in the combustion model of FPDEG [14]. The soot and NOx formation were calculated using the Hiroyasu-NSC model and the 12 steps NOx model separately.

The main parts of FPDEG experiment prototype include: two opposed-piston two-stroke FPEGs, high-pressure common rail system of diesel fuel, exhaust system, linear motor, motor control system, load system and test system. The experiment results of FPDEG experiment prototype can be found in literature [15-17]. **Figure 2** showed the calculation and experiment results of the in-cylinder pressure of the FPDEG. It was seen that the calculation results from the 3-D CFD FPDEG model were close to the experiment results, which proved the validity of the 3-D CFD FPDEG model.

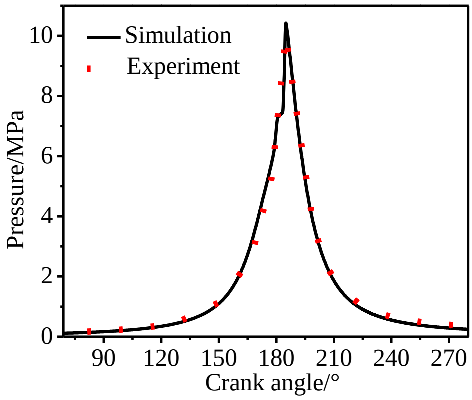

Figure 2. The calculation and experiment results of in-cylinder pressure

3. The effects of EGR rate on the combustion and emissions of FPDEG

Figure 3 and **Figure 4** showed the effects of EGR rate on the combustion and emissions of the FPDEG with the initial intake temperature of 345 K, equivalence ratio of 0.335, initial in-cylinder pressure of 0.114 MPa, and compression ratio of 20.2, separately. From the Figure 3, we can see that as the EGR rate increased (from 0 to 10%), the combustion phase lagged (the crank angle position of the first peak value was from 177° to 178°), peak value of heat release (from 312 J/° to 124 J/°), maximum in-cylinder temperature (from 2006 K to 1863 K) and in-cylinder pressure (from 13.8 MPa to 12.4 MPa) significantly decreased, and as the EGR rate was 20%, the HCCI combustion of FPDEG is an incomplete combustion, which was due to the increase of exhaust gas in the mixture. From the Figure 4, we can see that while the EGR rate increased (from 0 to 10%), the NOx content significantly decreased (from 1.08 g/kg fuel to 0.1 g/kg fuel), but SOOT content increased (from 0.004 g/kg fuel to 0.03 g/kg fuel), and as the EGR rate was 20%, due to the incomplete HCCI combustion, the UCH, CO and SOOT content were all high.

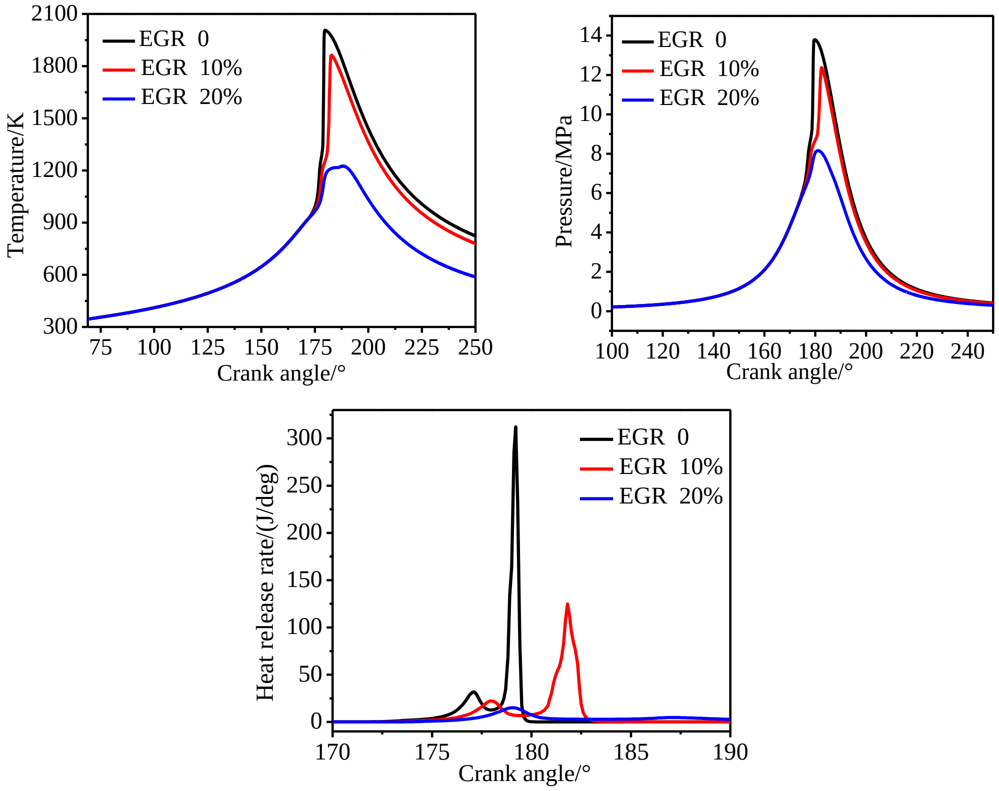

Figure 3. The effect of EGR rate on combustion

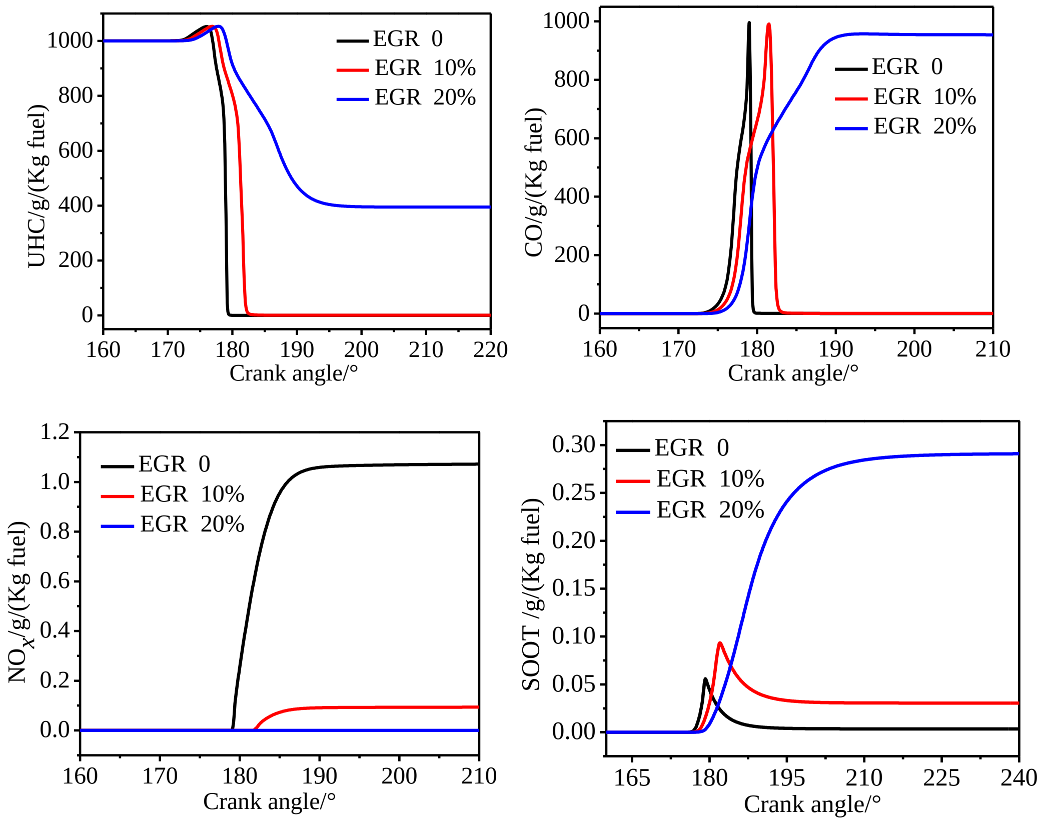

Figure 4. The effect of EGR rate on emissions

4. The effects of EGR rate on temperature and species concentration field distribution

Table 1-Table 4 demonstrated the calculated concentration field distribution in the cylinder of C7H8, C7H16, NO and CO respectively. **Table 5** showed the temperature field distribution in the cylinder. The CA10, the 10% cumulative heat release crank angle position, indicates the beginning of combustion. The CA50, the 50% cumulative heat release crank angle position, indicates the combustion phase. The CA90, the 90% cumulative heat release crank angle position, indicates the end of combustion.

Table 1. C7H8 concentration field distribution in the cylinder of FPDEG

EGR rate	CA10	CA50	CA90
0	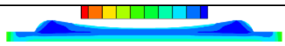	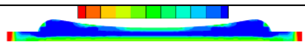	
10%	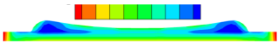	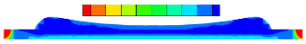	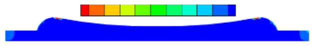
20%	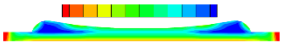	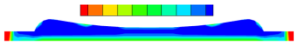	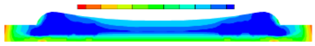

Table 2. C7H16 concentration field distribution in the cylinder of FPDEG

EGR rate	CA10	CA50	CA90
0	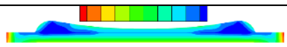		
10%	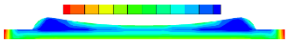	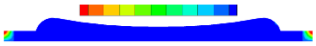	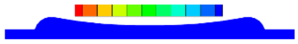
20%	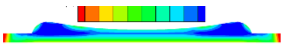	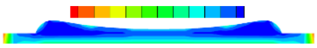	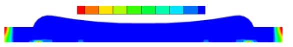

Table 3. CO concentration field distribution in the cylinder of FPDEG

EGR rate	CA10	CA50	CA90
0	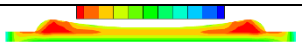	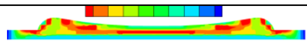	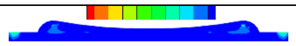
10%	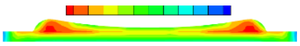	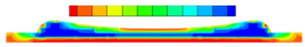	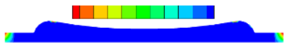
20%	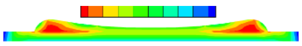	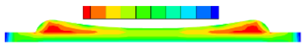	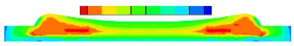

Table 4. NO concentration field distribution in the cylinder of FPDEG

EGR rate	CA10	CA50	CA90
0	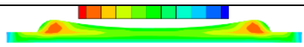	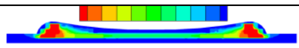	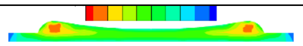
10%	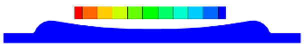	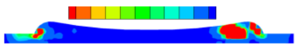	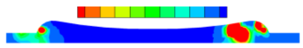
20%	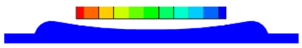	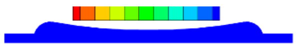	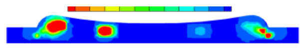

Table 5. The temperature field distribution in the cylinder of FPDEG

EGR rate	CA10	CA50	CA90
0	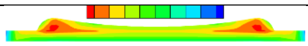	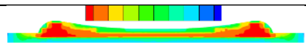	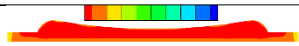
10%	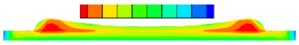	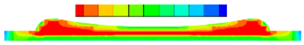	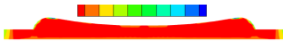
20%	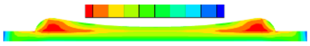	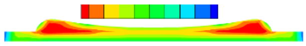	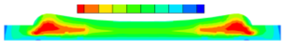

From **Table 1** to **Table 5**, we can see that, with the EGR rate of 0 and 10%, at the process of HCCI combustion, the temperature of the piston bowl was the maximum (about 1070 K), where the fuel (C7H8 and NC7H16) was first oxidized, while NO and CO were first produced; At the end of the HCCI combustion, the temperature, NO and CO concentration distribution were relatively uniform, and the fuel was completely consumed. However, with the EGR rate of 20%, the fuel (C7H8 and NC7H16) was not completely consumed, the temperature and CO concentration nearby piston bowl were the highest, and NO basically did not produce.

5. Conclusions

The simulation results of the 3-D CFD FPDEG showed that as the EGR rate increased (from 0 to 10%), the HCCI combustion phase of FPDEG slightly lagged, the peak value of heat release**,** the maximum in-cylinder temperature and pressure and the NOx content significantly decreased, but SOOT content increased. However, when the EGR rate was 20%, the HCCI combustion of FPDEG will be an incomplete combustion, and the UCH, SOOT and CO content all obviously increased. In addition, for the EGR rate of 0 and 10%, the temperature of the piston bowl was the maximum, where the fuel (C7H8 and NC7H16) was first oxidized, while the pollutants of NO and CO were first produced; at the end of the HCCI combustion, i.e. the CA90, the temperature (about 2000 K and 1850 K), NO and CO concentration distribution in the cylinder were relatively uniform, and the fuel (C7H8 and NC7H16) in the cylinder was completely consumed.

Acknowledgements

This work was supported by the Talent introduction Project of Anhui Science and Technology University (RCYJ201902) and the Key Excellent Young Teachers Program of Universities of Anhui Province (gxyqZD2019059).

References

[1] R.H. Thring, "Homogeneous-Charge Compression Ignition (HCCI) Engines", SAE Paper 892068, 1989.

[2] S. Onishi, S.H. Jo, K. Shoda, P.D. Jo, S. Kato, "Active Thermo-Atmosphere Combustion: A New Combustion Progress for Internal Combustion Engines", SAE Paper 790501, 1979.

[3] P.M. Najt, D.E. Foster, "Compression Ignited Homogeneous Charge Combustion", SAE Paper 830264, 1983.

[4] T.W. Ryan, T.J. Callahan, "Homogeneous Charge Compression Ignition of Diesel Fuel", SAE Paper 961160, 1996.

[5] M. Christensen, A. Hultqvist, B. Johansson, "Demonstrating the Multi-Fuel Capacity of a Homogeneous Charge Compression Ignition Engine with Variable Compression Ratio", SAE Paper, 1999-01-3679, 1999.

[6] Z.W. Zhang, H.H. Feng, Z.X. Zuo, "Numerical investigation of a free-piston hydrogen-gasoline engine linear generator", Energies, Vol. 13, No. 18, 2020, 4685, DOI: 10.3390/en13184685.

[7] C.Q. Li, Y.D. Wang, B.R. Jia, A.P. Roskilly, "Application of Miller cycle with turbocharger and ethanol to reduce NOx and particulates emissions from diesel engine - A numerical approach with model validations", Applied Thermal Engineering, Vol. 150, 2019, 904–911.

[8] M. Bergman, J. Fredriksson, V.I. Golovitchev, "CFD-based optimization of diesel-fueled free piston engine prototype for conventional and HCCI combustion", SAE Paper, 2008-01-2423, 2008.

[9] C.J. Chiang, J.L. Yang, S.Y. Lan, T.W. Shei, W.S. Chiang, B.L. Chen, "Dynamic modeling of a SI/HCCI free-piston engine generator with electric mechanical valves", Applied Energy, Vol. 102, 2013, 336-346.

[10] Tsolakis, A. Megaritis, M.L. Wyszynski, "Low temperature exhaust gas fuel reforming of hydrogen combustion engines", Fuel, Vol. 83, No. 13, 2004, 1837-1845.

[11] Y. Jamal, T. Wagner, M.L. Wyszynski, "Exhaust gas reforming of gasoline at moderate temperatures", International Journal of Hydrogen Energy, Vol. 21, No. 6, 507-519.

[12] D. Yap, S.M. Peucheret, A. Megaritis, M.L. Wyszynski, H.M. Xu, "Natural gas HCCI engine operation with exhaust gas fuel reforming", International Journal of Hydrogen Energy, Vol. 31, No. 5, 587-95, 2006.

[13] H.J. Curran, P. Gaffuri, W.J. Pitz, et al. "A comprehensive modeling study of n-heptane oxidation", Combustion and Flame, Vol. 114, No. 1-2, 1998, 149-177.

[14] H. Wang, M. Yao, Z. Yue, et al. "A reduced toluene reference fuel chemical kinetic mechanism for combustion and polycyclic-aromatic hydrocarbon predictions", Combustion and Flame, Vol. 162, No. 6, 2015, 2390-2404.

[15] Q. Zhang, Y. Wang, W. Lin, et al. "Contact mechanics analysis and optimization of shape modification of electric vehicle gearbox", Jordan Journal of Mechanical and Industrial Engineering, Vol. 14, No. 1, 2020, 15-24.

[16] H. Feng, C. Guo, C. Yuan, Y. Guo, Z. Zuo, A.P. Roskilly, B. Jia, "Research on combustion process of a free piston diesel linear generator", Applied Energy, Vol. 161, 2016, 395-403.

[17] M.B. Shongwe, O.O. Ajibola, M.E. Masonyaneng, et al. "Characterization and heat diffusion characteristics of spark plasma sintered Ni-50%Fe sintered alloy", Jordan Journal of Mechanical and Industrial Engineering, Vol. 13, No. 1, 2019, 61-67.